CHAPTER 1

INTRODUCTION

1.1 General

Our real world gives a lot of alternatives to meet the energy needs of humanity. One of them, which are as of now in the service of mankind, is the arrival of the binding energy of atomic nuclei. Energy is created by nuclear fission in nuclear power plants everywhere throughout the world. Nonetheless, manageable and sustainable energy production to the electricity grid by fusion reactions has not yet been accomplished.

1.2 Fusion power generation

A model of reliable fusion energy production is the Sun. Its hydrogen (^{1}H) fuel is changed over to helium (^{4}He) in diverse astrophysical reaction chains. These fusion reactions gave energy for several billions of years to life on Earth. In stellar cores the rate of fusion reactions is very moderate, in light of the fact that proton-neutron decays have to occur. Subsequently, astrophysical reaction chains have very low cross-sections, in this w ay the released power density of the Sun is less than 1 W/ m^3

Reproduction of stellar core conditions on Earth for nuclear fusion power generation would be wasteful and inefficient. With a specific end goal to accomplish adequately high power from fusion reactions for electricity production, light isotopes ought to be picked such as deuterium (^{2}H ≡ D), tritium (^{3}H ≡ T) or ^{3}He. Some of the fusion reactions conceivable with the previously stated isotopes are listed here:

$$D + D \Rightarrow {}^{3}He\ (0.82\ MeV) + n\ (2.45\ MeV),$$
$$D + D \Rightarrow T\ (1.01\ MeV) + p\ (3.02\ MeV),$$
$$\mathbf{D + T \Rightarrow {}^{4}He}(3.52\ MeV) + \mathbf{n}(14.1\ MeV),$$
$$D + {}^{3}He \Rightarrow {}^{4}He\ (3.66\ MeV) + p\ (14.6\ MeV).$$

Considering the reaction rates mentioned above, the most prosperous reaction on Earth is the deuterium-tritium (D-T) reaction. The reaction rate of D-T peaks at a lower temperature and at a higher value than other reactions generally considered for fusion energy.

A colossal amount of deuterium is accessible in nature, in light of the fact that there is 1 atom of deuterium for each 6700 particles of hydrogen in natural water assets. In addition to the colossal assets, deuterium can be effectively extracted at a minimal effort. However, assembling tritium is troublesome. Tritium is a radioactive isotope and it has a half-existence of 12.3 years. Therefore, tritium can be found in nature only in small quantities. Given that there is no functional tritium breeding technology which can fulfill the demand of an energy producing fusion reactor, the required tritium must be delivered by the reactor itself. Exploiting the fusion reaction produced neutrons; tritium can be delivered from lithium utilizing the accompanying procedures:

$$^{6}\mathrm{Li} + \mathrm{n}\ (\mathrm{thermal}) = {}^{4}\mathrm{He} + \mathrm{T}$$
$$^{7}\mathrm{Li} + \mathrm{n}\ (\mathrm{energetic}) = {}^{4}\mathrm{He} + \mathrm{T} + \mathrm{n}$$

.The fusion-born neutrons produce tritium by hitting the wall containing lithium. By the process the fuel of a fusion power plant is deuterium and lithium. Both of them are non-radioactive components and are accessible in extensive quantities on Earth.

The end product of the fusion reaction and the tritium breeding reaction are helium, accordingly neither the fuel, nor the end-product of the fusion and breeding cycle is radioactive. Fusion experiment with particle accelerator gave useful information to determine the cross sections of the previously stated reactions. However, sustainable energy generation with accelerators cannot be achieved. Since the cross-segment of Coulomb scattering is several orders of magnitude higher than the cross-segment of the fusion reaction. Accordingly, the most promising method is to heat the D-T fuel to adequately high temperature that the thermal velocities are high enough to sustain fusion reactions.

1.3 Magnetic confinement fusion

One way of confining the fuel with such high temperature is to utilize a magnetic field. At the temperatures important for the fusion reaction, the particles are ionized and the fuel is present in the plasma state. The charged particles begin their helical motion in the plane along the magnetic field. The circular portion of this motion in the plane perpendicular to the field line

is called Gyromotion. The helical motion is suitable to keep the plasma, because it doesn't permit the particles to move perpendicular to the magnetic field, however they are free to move parallel to the magnetic field. The issue of losses at the ends of a linear device can be settled by bending the magnetic field lines into a torus. Nonetheless, in a toroidal geometry, the magnetic field is non- homogeneous.

The strength of the magnetic field is inversely proportional to the distance which is measured from the center of the torus, because of the higher current density in the toroidal field coils in the internal side of the torus leads in a stronger magnetic field. This non-homogeneity prompts to a charge dependent drift (∇B drift), which causes the electrons and ions to drift in vertically opposite directions. The subsequent vertical electric field makes a charge free E×B drift, which moves the whole plasma towards the outside of the torus. This electric field between the top and the base of the torus can be shorted out by helically twisting the magnetic field lines.

A sort of magnetic confinement device is the tokamak, in which the magnetic field lines are helically twisted by plasma current. In tokamak geometry, the toroidal direction is the long way whereas the poloidal direction is the short way around the torus. The toroidal plasma current is driven by the transformer coil and it twists the magnetic field lines as it generates a poloidal magnetic field. The twist of magnetic field lines is depicted by the safety factor. The safety factor ***q*** is the ratio of toroidal transits per single poloidal transit of a magnetic field line. Because of the axisymmetric of a tokamak device, the magnetic field lines are composed into magnetic flux surfaces. Along the magnetic field lines, the particles move freely, thus the plasma parameters on the magnetic flux surfaces are adjusted very quickly, while the transport perpendicular to the surfaces is several orders of magnitude slower. In purpose to realize the self-sustaining magnetically confined plasma, the discharged fusion energy has to heat the plasma. The energy produced in a fusion reaction is dispersed as kinetic energy to the fusion products. As per their mass proportion, 80 % of the energy is conveyed by the neutrons which do not interact with the plasma and hit the plasma confronting part. The remaining 20 % energy is conveyed by the He nuclei. These He^{2+} ions have 3.5 MeV of initial energy and isotropic angular distribution. The self-heating provided by the He^{2+} ions (α-particles) is called α-heating. In the hot plasma the typical mean free path of fusion-born α-particles is very long compared to the size of the device. Thus, it is vital to well confine the high energy α-particles.

1.4 What is plasma

Matter defined in four state like solid, liquid, gas and plasma. Plasma is one of the most important crucial conditions of matter. Plasma has properties not at all like those of alternate states. Plasma is nothing but ionized gas; it can be made by heating a gas or subjecting it to an in number electromagnetic field connected with a laser or microwave generator. This abatements or builds the quantity of electrons, making positive or negative charged particles called ions and is joined by the separation of atomic bonds, if present. The vicinity of a noteworthy number of charge transporters makes plasma electrically conductive with the goal that it reacts emphatically to electromagnetic fields. Like gas, plasma does not have a distinct shape or a positive volume unless encased in a holder. Not at all like gas, affected by an attractive field, may it frame structures, for example, fibers, shafts and twofold layers.

Plasma is the most plentiful type of conventional matter in the Universe, the vast majority of which is in the thin intergalactic areas, especially the intracluster medium, and in stars, including the Sun. A typical type of plasmas on Earth is found in neon signs.

A great part of the comprehension of plasmas has originated from the quest for controlled atomic combination and combination power, for which plasma material science gives the investigative.

Chapter 2

Literature review

Role of dust in plasma is very useful research field in modern-day. It is play very important role for generation of electricity. It is also very important for safety procedure .a lot researcher involve in this field. We have following view of different researcher and their view.

Fisch [1] observed the continuous operation of a tokamak fusion reactor requires, among other things, a means of providing continuously the toroidal current. Such operation is preferred to the conventional pulsed operation, where the plasma current is induced by a time-varying magnetic field. A variety of methods have been proposed to provide continuous current, including methods that utilize particle beams or radio-frequency waves in any of several frequency regimes. Currents as large as half a mega-amp have now been produced in the laboratory by such means, and experimentation in these techniques has now involved major tokamak facilities worldwide.

Mukhovatov et al. [2] have observed ITER will be the first magnetic confinement device with burning DT plasma and fusion power of about 0.5 GW. Parameters of ITER plasma have been predicted using methodologies summarized in the ITER Physics Basis (1999 ***Nucl. Fusion*** **39** **2175**). During the past few years, new results have been obtained that substantiate confidence in achieving $Q \geq 10$ in ITER with inductive H-mode operation. These include achievement of a good H-mode confinement near the Greenwald density at high triangularity of the plasma cross section; improvements in theory-based confinement projections for the core plasma, even though further studies are needed for understanding the transport near the plasma edge; improvement in helium ash removal due to the elastic collisions of He atoms with D/T ions in the divertor predicted by modelling; demonstration of feedback control of neoclassical tearing modes and resultant improvement in the achievable β-values; better understanding of edge localized mode (ELM) physics and development of ELM mitigation techniques; and demonstration of mitigation of plasma disruptions. ITER will have a flexibility to operate also in steady-state and intermediate (hybrid) regimes. The 'advanced tokamak' regimes with weak or negative central magnetic shear and internal transport barriers

are considered as potential scenarios for steady-state operation. The paper concentrates on inductively driven plasma performance and discusses requirements for steady-state operation in ITER.

ITER Physics Expert Group on Energetic Particles [3] heating and current drive systems must fulfil several roles in ITER operating scenarios: heating through the H-mode transition and to ignition; plasma burn control; current drive and current profile control in steady state scenarios; and control of MHD instabilities. They must also perform ancillary functions, such as assisting plasma start-up and wall conditioning. It is recognized that no one system can satisfy all of these requirements with the degree of flexibility that ITER will require. Four heating and current drive systems are therefore under consideration for ITER: electron cyclotron waves at a principal frequency of 170GHz; fast waves operating in the range 40-70MHz (ion cyclotron waves); lower hybrid waves at 5GHz; and neutral beam injection using negative ion beam technology for operation at 1MeV energy. It is likely that several of these systems will be employed in parallel. The systems have been chosen on the basis of the maturity of physics understanding and operating experience in current experiments and on the feasibility of applying the relevant technology to ITER. Here, the fundamental physics describing the interaction of these heating systems with the plasma is reviewed, the relevant experimental results in the exploitation of the heating and current drive capabilities of each system are discussed, key aspects of their application to ITER are outlined, and the major technological developments required in each area are summarized.

Ikeda et al. [5] have observed the effects of the wave accessibility condition on lower hybrid current drive (LHCD) are investigated in JT-60U. The density dependence of the detectable maximum photon energy of hard X rays in LHCD plasmas is consistent with that of the maximum electron energy which is limited by the accessibility condition. The current drive efficiency and the driven current profile are affected by the accessibility condition. Inaccessible wave power enhances impurity content, particle recycling and main plasma radiation loss, and in extreme cases triggers a MARFE. The wave intensity on the plasma periphery, which is detected by a Langmuir probe located on the diverter plate, is also consistent with an inaccessible power fraction going into the plasma interior. A ray trace analysis taking account of toroidal effect indicates that the inaccessible wave power is localized on the plasma periphery and finally propagates into the diverter plasma region

Umeda et al. [8] have observed the injection performance of the negative-ion based NBI (N-NBI) system for JT-60U has been improved by correcting beamlet deflection and improving spatial uniformity of negative ion production. Beamlet deflection at the peripheral region of the grid segment due to the distorted electric field at the bottom of the extractor has been observed. This was corrected by modifying the surface geometry at the extractor to form a flat electric field. Moreover, beamlet deflection due to beamlet–beamlet repulsion caused by space charge was also compensated for byextruding the edge of the bottom extractor. This resulted in a reduction of the heat loading on the NBI port limiter. As a result of the improvement above, continuous injection of a 2.6 MW H^0 beam at 355 Kev has been achieved for 10 s. Thus, long pulse injection up to the nominal pulse duration of JT-60U was demonstrated. This has opened up the prospect of long pulse operation of the negative-ion based NBI system for a steady-state tokamak reactor. So far, a maximum injection power of 5.8 MW at 400 Kev with a deuterium beam, and 6.2 MW at 381 Kev with a hydrogen beam have been achieved in the JT-60U N-NBI. Uniformity of negative ion production was improved by tuning the filament emission current so as to direct more arc power into the region where less negative ion current was extracted. The resonant ion-beam—driven electrostatic ion-cyclotron instability is identified. Measured dispersion relation and onset versus beam energy and density agree with numerical calculations based on a theory which includes beam-acoustic terms. After amplitude saturation, velocity-space diffusion of the beam ions is observed.

Oikawa et al. [10] Observations of super thermal ion-cyclotron emission from JET Ohmic and neutral-beam-heated discharges is presented. Previously unobserved narrow-band spectral features correspond in both cases to multiple harmonics and half-harmonics of the proton gyro frequency at the outer edge of the plasma. In this region, fusion products with large radial excursions and injected fast ions produce anisotropic velocity distributions with positive perpendicular gradient. It is discussed how these may relax by maser action, giving rise to the observed localized radiation.

Cottrell et al. [12] have observed Super thermal ion cyclotron emission (ICE) is observed in both fusion and space plasmas. Typical spectra display strong peaks at sequential multiple ion cyclotron harmonics, and distinct energetic ion populations are present in the emitting regions. In JET and TFTR, for example, ICE appears to be driven by fusion products or by injected beam ions in the outer mid plane; and in the Earth's ring current, radiation belts, and bow shock, ICE has been observed by the spacecraft OGO 3, GEOS 1

and 2 and AMPTE/IRM, often in conjunction with highly non-Maxwellian proton populations. Common emission mechanisms, arising from collective relaxation of energetic ion populations, appear to operate in both the fusion and space plasma environments. These are reviewed, and the potential role of ICE as a diagnostic of energetic ion populations is also examined.

Dendy et al. [13] have observed Ion cyclotron emission (ICE) excited by collective instability of fusion α particles has been observed during deuterium-tritium experiments with radio-frequency heating and neutral beam injection (NBI) in the Joint European Torus. A model based on classical α-particle confinement is broadly consistent with this data. ICE spectra from discharges with high-power NBI also show evidence of ion hybrid wave excitation by beam ions, relevant to α channeling.

Chapter 3

ROLE OF DUST IN PLASMA

3.1Introduction

Smoke, mist, ash, fog, tidy all allude to particles that can be suspended in a fluid or a gas. Dusty media have dependably been of extensive hobby. The Egyptians utilized dust particles suspended in a fluid to make ink, the Chinese found their dangerous properties. Dust particles are still of real enthusiasm for an extensive variety of utilizations from dry powder coatings barometrical research to the microelectronics business. In any cases, these particles can be valuable then again hurtful and hence a great deal of studies is given to them.

Dusty plasmas are ionized gasses in which there are some charged naturally visible dust particles. They are extremely regular media and can be found in nature, for example, in an astrophysical environment or planetary upper climate as well as in human made plasma (laboratory or industrial discharges fusion plasmas)[38,39,40].

3.2 Dust in Environment

Dust particles have been found in numerous space situations and structure what is referred to as dusty plasma as they interface with space plasma. Dust alludes to a gathering of fine particles of nanometre to micrometre estimated which are made of metallic or non-metallic materials and are available in space either normally or as an aftereffect of human exercises. Normally, dust particles can be found in numerous astrophysical circumstances, for example, in the planetary ring of planets, for example, Saturn what's more, Jupiter, in cometary tails, in interstellar cloud and in an airless planetary bodies and space rock. Shuttle discharges, for example, from fuel and material debasement additionally add to the vicinity of dust particles in space. The communication between dust molecule and space plasma has created numerous intriguing phenomena and has turned into a noteworthy field of study in space material science. The investigation of dusty plasma has strengthened in the late twentieth century as a consequence of the early space investigations, specifically after the Apollo missions, and the development semiconductor industry. In the first case, dust particles experienced amid numerous of the missions have turned into a noteworthy issue to space vehicle working on the lunar surface and in addition on space explorer's life sparing types of gear. In the recent case, dust particles have been recognized as fundamental contaminant in wafer creation process which decides the wafer creation yields. In both cases, dust particles are presented to plasma making them get charge and in the long run get include in the general plasma framework[43].

3.3 History of dusty plasma

3.3.1 The early age

Before the 20th century, dusty plasmas were known as the zodiacal light and the noctilucent mists (found around a century back). Be that as it may, the material science of dusty plasmas did not begin before the perception of dust particles in a research facility release (hot cathode tube shaped positive section) by Irvin Langmuir in the 1920's. Tightening and insecurities of the plasma were watched and doled out to the vicinity of little clean particles originating from the sputtered tungsten cathode. From this time to the 1960's, the impact of dust and/or totals in low weight plasmas was sporadically studied the impact of dust particles in burning plasmas, (for example, ignition results of strong rockets, burning results of hydrocarbon flares in which carbon particles may have framed, wake of a re-entry body) was mulled over in the 1950's and 1960's.. In the vast majority of these cases, the dust particles radiate electrons thermionically (due a high dust molecule surface temperature), and in this way, their consequences for the plasma are not the same as the non-emitting dust particles that can be found in most low weight and low temperature plasmas. In the late 1960's, the impact of dust on DC positive sections picked up consideration once more. The impact of adversely charged expansive dust particles in a DC positive segment was explored. It was found that the dust molecule impact can be contrasted with the impact of negative particles in electronegative releases. These results can be summarized in following way

i) When the dust thickness is not very high and when every dust molecule can be considered as secluded, electron and particle densities can be concluded from the essential plasma comparisons in which a term relating to volume misfortunes on dust molecule surfaces is included (dust particles go about as surface ionization sinks). Additionally, the electron temperature and the pivotal electric field were observed to be higher than in a without dust section.

ii)When the dust thickness is high, the dust particles removes the wall of discharge and the plasma can be generally regarded as an arrangement of parallel plasma fibers between retaining dividers with a span about the request of the a large portion of the mean interparticle separation

iii) The dust molecule surface temperature will be more noteworthy than that of the gas because of its warming by surface recombination.

iv)The spiral conveyance of dust particles changes starting with one release then onto the next and is a trade-off between a Maxwell-Boltzmann conveyance, the impact because of

neighborhood or expansive scale gas development, the concoction obliteration of the molecule and the particle drag constrain in a firmly inhomogeneous discharge[43,44].

3.3.2 Astrophysical

The investigations of plasma-dust communications are of significant enthusiasm for astronomy as dusty plasmas can be discovered all over the place in a space domain and their physical properties should be comprehended to clarify perceptions.

In this way, a help to the material science of dusty plasma originated from astronomy with the revelation of

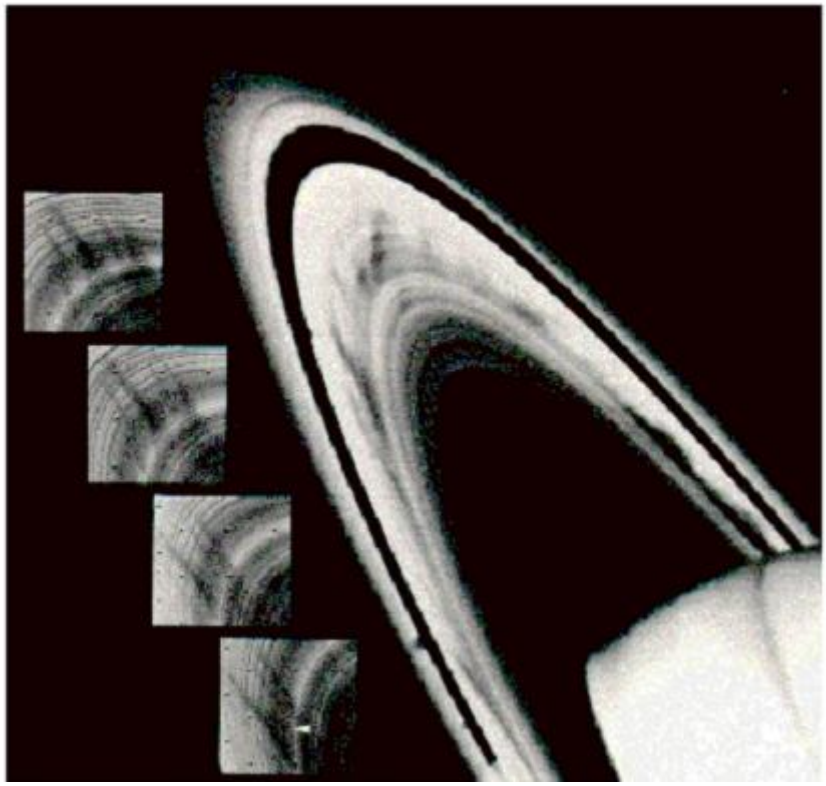

Fig 3.1 spokes" on Saturn's B ring [48]

nearly spiral spooky like "spokes" in the external bit of Saturn's B ring in the mid 1980's by the Voyager space tests (Fig.3.1). It presented a great deal of hypothetical works about plasma-dust cooperation in astrophysical situation.

3.3.3 The industrial period

In the late 1980's, dust molecule development was seen in research centre and mechanical synthetically dynamic discharges (Fig.3.2). Dust molecule growth in a modern reactor can be a noteworthy issue: dust particles falling on wafers (when the discharges are killed) can antagonistically influence the execution of semiconductor gadgets or the nature of slim film. Therefore the instrument of Growth of dust particles in plasmas should have been be

effectively mulled over. It was without a doubt a noteworthy issue to see how tidy particles were framed in the plasma and how to restrain their growth keeping in mind the end goal to stay away from issues amid modern procedures. For this reason, a great deal of works has been completed to comprehend the dust growth system. Dust growth occurs following a well-defined pattern

i. Arrangement of sub-atomic antecedents from gas separation

ii. Arrangement and aggregation of Nano crystallites from these antecedents

iii. Collection of the Nano crystallites

iv. Growth by sub-atomic staying

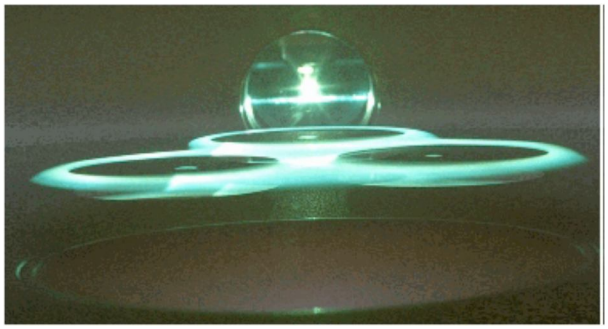

Fig.3.2 [47]

3.4 Charge and charge distribution

The molecule charge controls the dust elements both in lab and mechanical plasma reactors, furthermore in space plasmas. Therefore one of the principle challenges in dusty plasma is to comprehend the charging of dust particles in an extensive variety of test conditions, which incorporates mechanical also, space plasmas. Case in point, in most modern procedures in the microelectronics business, which utilizes silane as the receptive gas, dust defilement is a key issue. The dust progress furthermore, coagulation in space plasma is likewise phenomena represented by dust molecule charges

Elementary procedures prompting dust molecule charging are the accumulation of the particles and the electrons of the encompassing plasma, the associations with photons, auxiliary electron emanation due to impacts with vivacious particles, thermionic emanation, and so on. In research facility plasmas, charging by particle and electron accumulation is the common impact. Two amazing cases can be considered. At the point when the λ_D length of the dusty plasma is much smaller than the intergrain distance (a), the dust particles can be

considered as disconnected in the plasma. At the point when the λ_D is bigger than the intergrain distance (a), the dust particles interface with one another and have an aggregate conduct. The span of the dust molecule thought about to the Debye length additionally has an impact. Here, we consider just the situation where $r_d \leq \lambda_D$ where r_d is the range of the dust particles [35].

3.5 The Debye length

An essential attributes of plasmas is the screening of electric field made by individual charged (particles, electrons and dust particles) or by a surface with a potential that is diverse to the plasma potential. This screening impact has a characteristic length: the Debye length. This is the length beneath which the electric field of charged particles can impact the other charged molecule. In dusty plasmas, the linearized Debye length [35] is given by

$$\lambda_D = \frac{\lambda_{De}\lambda_{Di}}{\sqrt{\lambda_{De}^2 + \lambda_{Di}^2}}$$

$$\lambda_{Di(e)} = \sqrt{\frac{\varepsilon_0 K_B T_{i(e)}}{n_{i(e)0} e^2}}$$

Where $\lambda_{Di(e)}$ is the ion (electron) Debye length defined as

3.6 Example of instabilities observed in dusty plasmas

In plasmas, a wide mixed bag of waves exists because of coherent movement of the diverse plasma species (Langmuir waves and particle acoustic waves for example). In dusty plasmas, the charged dust grains change the wave engendering because of inhomogeneity in the dust conveyance, the adjusted quasi-neutrality condition and a few contemplations about dust molecule flow. Two significant subclasses of waves exist in mind boggling plasma. Two major subclasses of waves exist in dusty plasma:

i. Waves and oscillations emerging from the aggregate movement of the plasma (ion or electrons) and influenced by the dust particles

ii. Waves and oscillations because of the aggregate movement of the dust particles in different dust structures (dust cloud, fluids or precious stones) [35, 36].

3.6.1Dust Acoustic waves (DAWs)

The DA waves originate from the aggregate movement of the dust grains. The DA wave speed is much smaller than the ion and electron thermal speeds and subsequently ion and electron inactivity can be dismissed and the DA wave potential can be thought to be in harmony. The weight angle can be expected as adjusted by the electric power and

consequently the particle and electron circulations are Boltzmann dispersions. The reclamation constrain in the DA waves originates from the ion and electron (considered without inertia) weight while the dust molecule mass gives the wave inertial backing.

3.6.2 Dust-ion acoustic waves (DIAWs)

The DIA waves originate from the aggregate movement of the particles influenced by the vicinity of the dust particles. For adversely charged dust particles (ni0 > ne0), the DIA wave phase speed (w k) is more prominent than the particle ion velocity. It can be clarified by an increment of the electron Debye length because of electron losses on dust particles. Therefore, the electric filled $E = -\nabla\phi$ is larger. As $kv_{ti} \le w \le kv_{te}$ Landau damping of DIA waves is negligible.

3.6.3 Other waves and instabilities

Different mixtures of waves can be found in dusty plasma (from individual motions of dust particles in sheaths of gas discharge to compressional waves in dust gems) and their properties (instabilities, damping, and so forth.) rely on upon the plasma parameters .instability can likewise act naturally energized in dusty plasmas. In this way, it has been accounted for that the development of dust particles in plasma can trigger a few insecurities [43].

CHAPTER 4
ROLE OF DUST GRAINS

4.1Dusty Plasma Characteristics

Essential parameters of dusty plasma incorporate dust grain radius (r_d), average distance between grains (a), plasma Debye radius λ_D and the dust cloud measurement. Two unique administrations are remembered; (i) a segregated dust where $r_d \ll \lambda_D \leq a$ and

(ii) Gathering dust grain where $r_d \ll a \ll \lambda_D$ the previous case is alluded to as dust-in-plasma where dust particles are electrically confined from one another and take after a test inundated in plasma. The recent is known as dusty plasma where particles are firmly stuffed and their properties can be depicting all in all [48].

4.1.1-Macroscopic Neutrality

In a vast scale, dusty plasma is said to be electrically neutral. Without outer strengths, quasineutrality is seen at equilibrium which can be expressed as

$$q_i n_{i0} = e n_{e0} - q_d n_{d0} ,$$

Where n_{i0}, n_{e0} and n_{d0} are the density for ion, electron and dust respectively and $q_i = Z_{ie}$ is the charge for the ion species where Z_i = 1 for singly charged ion while $q_d = Z_{de}(-Z_{de})$ is dust charge where Z_d is the dust charge number. The number of charge Z_d on a dust molecule can fluctuate from few unit charges to thousands of unit charge contingent upon plasma parameters, dust density and the prevailing charging current. The charged dust changes the aggregate conduct of the plasma which incorporates permitting the development of electric field inside of the plasma, changing nearby plasma potential profile, altering molecule directions in the plasma, and changing and presenting new plasma waves, for example, dust acoustic waves and dust particle acoustic waves

4.1.2-Debye shielding

$$\nabla^2 \phi = \frac{\rho_q}{\varepsilon_0} = \frac{e}{\varepsilon_0}(n_e - n_i - q_d n_d)$$

Solution of above equation

$$\nabla^2 \phi = \left(\frac{1}{\lambda_{De}^2} + \frac{1}{\lambda_{Di}^2} \right) \phi$$

Where λ_{De}^2 and λ_{Di}^2 are the electron and ion Debye length given by

$$\lambda_{Di} = \sqrt{\frac{\varepsilon_0 K_B T_i}{n_{i0} e^2}} \quad , \quad \lambda_{De} = \sqrt{\frac{\varepsilon_0 K_B T_e}{n_{e0} e^2}}$$

The dusty plasma Debye length is given by

$$\lambda_D = \frac{\lambda_{De}\lambda_{Di}}{\sqrt{\lambda_{De}^2 + \lambda_{Di}^2}}$$

Where the dominant length depends on dust grain charge in a negatively charge dust grains, the lack of free electrons means $n_{e0} \leq n_{i0}$ which results in $\lambda_{De} \gg \lambda_{Di}$ consequently, $\lambda_{De} \simeq \lambda_{Di}$, In a positively charged dusty plasma $\lambda_{De} \ll \lambda_{Di}$ [35,36].

4.1.2 Characteristic Frequencies

Dust plasma frequency can be derived in a similar fashion as in equation in cold, unmagnetized dusty plasma [48].

$$\omega_p^2 = \sum_s \omega_{ps}^2$$

Where s = i, e and d for electrons, ions and dust respectively and dust plasma frequency given by

$$\omega_{p,d}^2 = \frac{n_d Z_d^2 e^2}{\varepsilon_0 m_d}$$

Where the charge of the dust is taken into account in the calculation

4.2Dust Charging Process

The dust charging procedure can be portrayed by three basic procedures;

(i) Communication with encompassing plasma particles,

(ii) Connection with enthusiastic plasma particles

(iii) Communication with photons from sun based UV. Dust charging happens

at the point when the surface tries to adjust the present entering and leaving the surface. At this express the dust is thought to be in equilibrium, and the surface is charged to what is known as skimming potential.

The entire procedure can be summed up by the present offset mathematical statement, i.e.

$$\sum I_i + I_e + I_{ph} + I_{\sec} = 0$$

Where I_e and I_i are the current by the surrounding plasma (electrons and ions), I_{ph} is Photoelectron current and $I_{\sec}$ is the optional outflow current because of cooperation with enthusiastic plasma particles. The charging level will then rely on upon the overwhelming current streaming all through the dust molecule which causes the dust to charge to either positive or negative [48].

Chapter 5

MATHEMETICAL MODELLING IN PRESENCE OF DUST GRAINS

The dust grain perturbation [34] is given by

$$n_{d1r} = \frac{n_{d0r} Q_{d0r} \phi k^2}{m_d \omega^2} \quad , \tag{1}$$

where m_d is mass of dust grains

In the present case, dust is treated as unmagnetized because $\omega \sim \omega_{ci} \gg \omega_{cd}$ with $\omega_{cd} = \frac{Q_{do} B}{m_d c}$ being the dust gyrofrequency. Now applying probe theory to dust grain, the charge on a dust grain Q_d is known to be balanced with the plasma currents on the grain surface as [34]

$$\frac{dQ_{d1r}}{dt} = I_{er} + I_{ir} \tag{2}$$

Equation (2) can be rewritten as

$$\frac{dQ_{d1r}}{dt} + \eta_r Q_{d1r} = I_{e0r} \left(\frac{n_{ir}}{n_{i0}} - \frac{n_{er}}{n_{e0}} \right) \tag{3}$$

where $\eta_r = 10^{-2} \omega_{pr} \left(\frac{n_{e0}}{n_{i0}} \right) \left(\frac{a}{\lambda_D} \right)$ is the charging rate

(ω_{pr} is plasma frequency and λ_D is the Debye length)

Above equation demonstrates that charge changes on dust particles are driven by the distinction in relative density variances of ions and electrons and have a natural decay rate. Physically, the charge fluctuations decay the fact that any deviation of the grain potential from the equilibrium floating potential is restricted by electron and/or ion current into the grain.

Using $\frac{d}{dt} = -i\omega$ in equation (3), we get

$$Q_{d1r} = \frac{iI_{e0r}}{(\omega + i\eta_r)} \left(\frac{n_{ir}}{n_{i0}} - \frac{n_{er}}{n_{e0}} \right),$$

Q_{d1r} Can be rewritten after putting the value of n_{ir} and n_{er} [33]

$$Q_{d1r} = -\frac{i\left(\frac{I_{e0r}k^2}{4\pi e n_{e0}}\right)}{(\omega + i\eta_r)}\left(X_{er}(\phi + \phi_{pr}) + X_{ir}\frac{n_{e0}}{n_{i0}}\right) \quad (4)$$

where $X_{er} \approx \frac{2\omega_{pr}^2}{k^2 V_{ther}^2} = \frac{\omega_{pir}^2 m_i}{k^2 c_{sr}^2 m}$, $\quad X_{ir} = \frac{2\omega_{pir}^2}{k^2 V_{thir}^2}\left[1 - I_0 e^{-b_i} - \frac{\omega_{ci} I_1 e^{-bi}}{\omega - \omega_{ci}}\right]$

Poisson's equation

$$\nabla^2\phi = 4\pi e n_{er} - 4\pi e n_{ir} - 4\pi e n_{br} - 4\pi n_{d0r} Q_{d1r} - 4\pi n_{d1r} Q_{d0r}$$

Substituting the value of n_{er}, n_{ir}, n_{br} [33] and Q_{d1r}, n_{d1r} from Eqs. (1), (4), we get

$$\left[1 + X_{er}\left(1 + \frac{i\beta_r}{(\omega + i\eta_r)}\right) + X_{ir}\left(1 + \frac{i\beta_r}{(\omega + i\eta_r)}\frac{n_{e0}}{n_{i0}}\right) + X_{br} + X_{dr}\right]\phi = -X_{er}\left(1 + \frac{i\beta_r}{(\omega + i\eta_r)}\right)\phi_{pr}$$

$$\varepsilon\phi = -X_{er}\left(1 + \frac{i\beta_r}{(\omega + i\eta_r)}\right)\phi_{pr} \quad , \quad (5)$$

where

$$\beta_r = \frac{I_{e0r}}{e}\left(\frac{n_{d0r}}{n_{e0}}\right), \quad X_{dr} = -\frac{\omega_{pdr}^2}{\omega^2} \quad , \omega_{pdr}^2 = \left(\frac{4\pi n_{d0r} Q_{d0r}^2}{m_d}\right)$$

$$\varepsilon = \left[1 + X_{er}\left(1 + \frac{i\beta_r}{(\omega + i\eta_r)}\right) + X_{ir}\left(1 + \frac{i\beta_r}{(\omega + i\eta_r)}\frac{n_{e0}}{n_{i0}}\right) + X_{br} + X_{dr}\right]$$

5.1 GROWTH RATE IN PRESENCE OF DUST GRAINS

ϕ_1 , ϕ_2 and ϕ_{pr} can be written after following Kumar and Tripathi [33]

$$\phi_1 = (\varepsilon - X_{er})k^2 k_\perp \bullet V_{0\perp}^* \frac{\phi}{k_1^2 \varepsilon_1}$$

$$\phi_2 = (\varepsilon - X_{er})k^2 k_\perp \bullet V_{0\perp} \frac{\phi}{k_2^2 \varepsilon_2}$$

$$\phi_{pr} = -\frac{e\phi_0}{2m\omega_{cr}^2 ik_z\omega_0}\left\{\left[K_\perp \bullet K_{0\perp} \times \omega_{cr}\left(\omega_0 k_{2z} - \omega_2 k_{0z}\right)\right]\frac{\left(\varepsilon - X_{er}\right)k^2 k_\perp \bullet V_{0\perp}\dfrac{\phi}{k_2^2\varepsilon_2}}{\omega_2}\right\}$$

$$-\frac{e\phi_0}{2m\omega_{cr}^2 ik_z\omega_0}\left\{\left[K_\perp \bullet K_{0\perp} \times \omega_{cr}\left(\omega_0 k_{1z} - \omega_1 k_{0z}\right)\right]\frac{\left(\varepsilon - X_{er}\right)k^2 k_\perp \bullet V_{0\perp}^*\dfrac{\phi}{k_1^2\varepsilon_1}}{\omega_1}\right\} \qquad (6)$$

Substituting the equation (6) in equation (5), we get

$$\varepsilon = \mu_r\left[\frac{1}{\varepsilon_1} + \frac{1}{\varepsilon_2}\right] \quad , \qquad (7)$$

where

$$\mu_r = -X_{er}\left(\varepsilon - X_{er}\right)\left(1 + \frac{i\beta_r}{\left(\omega + i\eta_r\right)}\right)\frac{k^2 \sin\delta_r U^2\left(1-\Delta_1\right)}{4\omega_1^2}$$

where

$$\Delta_1 = \frac{\omega k_{0\|}}{\omega_0 k_\|}, \qquad U = -\frac{ek_0\phi_0}{m\omega_{cr}}$$

δ_r is the angle between K_1 and $K_{0\perp}$

$$\varepsilon_1 = 1 + \frac{\omega_{pr}^2}{\omega_{cr}^2} - \frac{\omega_{pr}^2}{\omega_1^2}\frac{\left(k_z - k_{0z}\right)^2}{k_{0\perp}^2 + k_\perp^2} - \frac{\omega_{pir}^2}{\omega_1^2}$$

Putting $\omega_{pr}^2 = \omega_{pir}^2\dfrac{m_i}{m}$, we get

$$\varepsilon_1 = 1 + \frac{\omega_{pr}^2}{\omega_{cr}^2} - \frac{\omega_{pir}^2 m_i}{\omega_1^2 m}\frac{\left(k_z - k_{0z}\right)^2}{k_{0\perp}^2 + k_\perp^2} - \frac{\omega_{pir}^2}{\omega_1^2}$$

$\omega_1 = \omega - \omega_0$

$k_1 = k - k_0$

$k_{1z} = k_z - k_{0z}$

$\omega_0 \geq \omega$

$\omega_1 = -\omega_0$

$\omega_2 = \omega_0$

$k_{0z} \geq k_z$

$$\omega_o^2 = \omega_{LH}^2\left(1+\frac{k_{oz}^2 m_i}{k_0^2 m}\right)$$

$$\omega_{LH}^2 = \omega_{pir}^2\left(1+\frac{\omega_{pr}^2}{\omega_{cr}^2}\right)^{-1}$$

$$\varepsilon_1 = -\frac{2\omega}{\omega_0}\left(1+\frac{\omega_{pr}^2}{\omega_{cr}^2}\right)+\left(1-\frac{\omega_{LH}^2}{\omega_0^2}\right)\left(\frac{2k_z}{k_{0z}}+\frac{k_\perp^2}{k_{0\perp}^2}\right)\left(1+\frac{\omega_{pr}^2}{\omega_{cr}^2}\right)$$

Here we assume

$$\alpha_{3r} = \left(1-\frac{\omega_{LH}^2}{\omega_0^2}\right)\left(\frac{k_\perp^2}{k_{0\perp}^2}\right)$$

$$\beta_{3r} = \left(1-\frac{\omega_{LH}^2}{\omega_0^2}\right)\left(\frac{2k_z}{k_{0z}}\right)$$

$$\varepsilon_1 = -\frac{2}{\omega_0}\left(1+\frac{\omega_{pr}^2}{\omega_{cr}^2}\right)\left[\omega-\frac{\omega_0}{2}\left(\alpha_{3r}+\beta_{3r}\right)\right] \tag{8}$$

Similarly we get

$$\varepsilon_2 = \frac{2}{\omega_0}\left(1+\frac{\omega_{pr}^2}{\omega_{cr}^2}\right)\left[\omega-\frac{\omega_0}{2}\left(\beta_{3r}-\alpha_{3r}\right)\right] \tag{9}$$

$$\frac{1}{\varepsilon_1}+\frac{1}{\varepsilon_2} = -\frac{\omega_0^2\frac{\alpha_{3r}}{2}}{\left(1+\frac{\omega_{pr}^2}{\omega_{cr}^2}\right)\left[\left(\omega-\frac{\omega_0}{2}\left(\alpha_{3r}+\beta_{3r}\right)\right)\left(\omega-\frac{\omega_0}{2}\left(\beta_{3r}-\alpha_{3r}\right)\right)\right]}$$

Substituting the value of equation (8) and (9) in equation (7) and we get

$$\varepsilon = -\frac{\mu_r\omega_0^2\frac{\alpha_{3r}}{2}}{\left(1+\frac{\omega_{pr}^2}{\omega_{cr}^2}\right)\left[\left(\omega-\frac{\omega_0}{2}\left(\alpha_{3r}+\beta_{3r}\right)\right)\left(\omega-\frac{\omega_0}{2}\left(\beta_{3r}-\alpha_{3r}\right)\right)\right]}$$

Let $\varepsilon = \left[1+X_{er}\left(1+\frac{i\beta_r}{(\omega+i\eta_r)}\right)+X_{ir}\left(1+\frac{i\beta_r}{(\omega+i\eta)_r}\frac{n_{e0}}{n_{i0}}\right)+X_{br}+X_{dr}\right]$ and we get

$$\left[1+X_{er}\left(1+\frac{i\beta_r}{(\omega+i\eta_r)}\right)+X_{ir}\left(1+\frac{i\beta_r}{(\omega+i\eta_r)}\frac{n_{e0}}{n_{i0}}\right)+X_{br}+X_{dr}\right]$$

$$+\frac{\mu_r\omega_0^2\frac{\alpha_{3r}}{2}}{\left(1+\frac{\omega_{pr}^2}{\omega_{cr}^2}\right)\left[\left(\omega-\frac{\omega_0}{2}\left(\alpha_{3r}+\beta_{3r}\right)\right)\left(\omega-\frac{\omega_0}{2}\left(\beta_{3r}-\alpha_{3r}\right)\right)\right]}=0$$

$$1+\frac{\omega_{pir}^2 m_i}{k^2c_{sr}^2 m}\left(1+\frac{i\beta_r}{(\omega+i\eta_r)}\right)+\frac{2\omega_{pir}^2}{k^2V_{thir}^2}\left[1-I_0e^{-b_i}-\frac{\omega_{ci}I_1e^{-bi}}{\omega-\omega_{ci}}\right]\left(1+\frac{i\beta_r}{(\omega+i\eta_r)}\frac{n_{e0}}{n_{i0}}\right)$$

$$-\frac{\omega_{pdr}^2}{\omega^2}+\frac{\alpha_2}{\left(\omega-k_zV_{0bz}-\omega_{cbr}\right)^2}+\frac{\mu_r\omega_0^2\frac{\alpha_{3r}}{2}}{\left(1+\frac{\omega_{pr}^2}{\omega_{cr}^2}\right)\left[\left(\omega-\frac{\omega_0}{2}\left(\alpha_{3r}+\beta_{3r}\right)\right)\left(\omega-\frac{\omega_0}{2}\left(\beta_{3r}-\alpha_{3r}\right)\right)\right]}=0$$

$b_i \ll 1, I_0 \ll 1, \quad \left(1-I_0e^{-b_i}\right)\simeq 1$,we get

$$\frac{2\omega_{pir}^2}{k^2V_{thir}^2}\left[1-I_0e^{-b_i}-\frac{\omega_{ci}I_1e^{-bi}}{\omega-\omega_{ci}}\right]=\frac{2\omega_{pir}^2}{k^2V_{thir}^2}\left[1-\frac{\omega_{ci}I_1e^{-bi}}{\omega-\omega_{ci}}\right]$$

$$1+\frac{\omega_{pir}^2 m_i}{k^2c_{sr}^2 m}\left(1+\frac{i\beta_r}{(\omega+i\eta_r)}\right)+\frac{2\omega_{pir}^2}{k^2V_{thir}^2}\left[1-\frac{\omega_{ci}I_1e^{-bi}}{\omega-\omega_{ci}}\right]\left(1+\frac{i\beta_r}{(\omega+i\eta_r)}\frac{n_{e0}}{n_{i0}}\right)$$

$$-\frac{\omega_{pdr}^2}{\omega^2}+\frac{\alpha_2}{\left(\omega-k_zV_{0bz}-\omega_{cbr}\right)^2}+\frac{\mu_r\omega_0^2\frac{\alpha_{3r}}{2}}{\left(1+\frac{\omega_{pr}^2}{\omega_{cr}^2}\right)\left[\left(\omega-\frac{\omega_0}{2}\left(\alpha_{3r}+\beta_{3r}\right)\right)\left(\omega-\frac{\omega_0}{2}\left(\beta_{3r}-\alpha_{3r}\right)\right)\right]}=0$$

Or

$$1+\frac{\omega_{pir}^2 m_i}{k^2c_{sr}^2 m}+\frac{2\omega_{pir}^2}{k^2V_{thir}^2}+\frac{\omega_{pir}^2 m_i}{k^2c_{sr}^2 m}\left(\frac{i\beta_r}{(\omega+i\eta_r)}\right)-\frac{2\omega_{pir}^2}{k^2V_{thi_r}^2}\left(\frac{\omega_{ci}I_1e^{-bi}}{\omega-\omega_{ci}}\right)$$

$$+\frac{2\omega_{pir}^2}{k^2V_{thir}^2}\left(\frac{i\beta_r}{(\omega+i\eta_r)}\frac{n_{e0}}{n_{i0}}\right)-\frac{2\omega_{pir}^2}{k^2V_{thir}^2}\left(\frac{\omega_{ci}I_1e^{-bi}}{\omega-\omega_{ci}}\right)\left(\frac{i\beta_r}{(\omega+i\eta_r)}\frac{n_{e0}}{n_{i0}}\right)-\frac{\omega_{pdr}^2}{\omega^2}$$

$$= -\left[\frac{\alpha_2}{\left(\omega - k_z V_{0bz} - \omega_{cbr}\right)^2} + \frac{\mu_r \omega_0^2 \frac{\alpha_{3r}}{2}}{\left(1 + \frac{\omega_{pr}^2}{\omega_{cr}^2}\right)\left[\left(\omega - \frac{\omega_0}{2}\left(\alpha_{3r} + \beta_{3r}\right)\right)\left(\omega - \frac{\omega_0}{2}\left(\beta_{3r} - \alpha_{3r}\right)\right)\right]} \right]$$

Let

$$A_1 = \left(\omega - k_z V_{0bz} - \omega_{cbr}\right)^2$$

$$B_1 = \frac{\mu_r \omega_0^2 \frac{\alpha_{3r}}{2}}{\left(1 + \frac{\omega_{pr}^2}{\omega_{cr}^2}\right)}$$

$$C_1 = \left[\left(\omega - \frac{\omega_0}{2}\left(\alpha_{3r} + \beta_{3r}\right)\right)\left(\omega - \frac{\omega_0}{2}\left(\beta_{3r} - \alpha_{3r}\right)\right)\right]$$

$$S = \frac{2\omega_{pir}^2}{k^2 V_{thir}^2}$$

$$1 + \frac{\omega_{pir}^2 m_i}{k^2 c_{sr}^2 m} + \frac{2\omega_{pir}^2}{k^2 V_{thir}^2} + \frac{\omega_{pir}^2 m_i}{k^2 c_{sr}^2 m}\left(\frac{i\beta_r}{\left(\omega + i\eta_r\right)}\right) - \frac{2\omega_{pir}^2}{k^2 V_{thir}^2}\left(\frac{\omega_{ci} I_1 e^{-bi}}{\omega - \omega_{ci}}\right)$$

$$+ \frac{2\omega_{pir}^2}{k^2 V_{thir}^2}\left(\frac{i\beta_r}{\left(\omega + i\eta_r\right)}\frac{n_{e0}}{n_{i0}}\right) - \frac{2\omega_{pir}^2}{k^2 V_{thir}^2}\left(\frac{\omega_{ci} I_1 e^{-bi}}{\omega - \omega_{ci}}\right)\left(\frac{i\beta_r}{\left(\omega + i\eta_r\right)}\frac{n_{e0}}{n_{i0}}\right) - \frac{\omega_{pdr}^2}{\omega^2}$$

$$= -\left[\frac{\alpha_2}{A_1} + \frac{B_1}{C_1}\right]$$

Now we divide by S on both sides, we get

$$\frac{1 + \frac{\omega_{pir}^2 m_i}{k^2 c_{sr}^2 m} + \frac{2\omega_{pir}^2}{k^2 V_{thir}^2} + \frac{\omega_{pir}^2 m_i}{k^2 c_{sr}^2 m}\left(\frac{i\beta_r}{\left(\omega + i\eta_r\right)}\right)}{\frac{2\omega_{pir}^2}{k^2 V_{thir}^2}} + \frac{\frac{\omega_{pir}^2 m_i}{k^2 c_{sr}^2 m}\left(\frac{i\beta_r}{\left(\omega + i\eta_r\right)}\right)}{\frac{2\omega_{pir}^2}{k^2 V_{thir}^2}}$$

$$-\left(\frac{\omega_{ci}I_1e^{-bi}}{\omega-\omega_{ci}}\right)+\left(\frac{i\beta_r}{(\omega+i\eta_r)}\frac{n_{e0}}{n_{i0}}\right)-\left(\frac{\omega_{ci}I_1e^{-bi}}{\omega-\omega_{ci}}\right)\left(\frac{i\beta_r}{(\omega+i\eta_r)}\frac{n_{e0}}{n_{i0}}\right)-\frac{\omega_{pdr}^2}{S\omega^2}$$

$$=-\frac{1}{S}\left[\frac{\alpha_2}{A_1}+\frac{B_1}{C_1}\right]$$

$$\frac{1+\dfrac{\omega_{pir}^2m_i}{k^2c_{sr}^2m}+\dfrac{2\omega_{pir}^2}{k^2V_{thir}^2}}{\dfrac{2\omega_{pir}^2}{k^2V_{thir}^2}}=1+\frac{T_i}{T_e}+\frac{k^2V_{thir}^2}{2\omega_{pir}^2}=1+\Delta_r$$

$$\frac{\dfrac{\omega_{pir}^2m_i}{k^2c_{sr}^2m}\left(\dfrac{i\beta_r}{(\omega+i\eta_r)}\right)}{\dfrac{2\omega_{pir}^2}{k^2V_{thir}^2}}=\frac{T_i}{T_e}\left(\frac{i\beta_r}{(\omega+i\eta_r)}\right)$$

$$1+\Delta_r+\frac{T_i}{T_e}\left(\frac{i\beta_r}{(\omega+i\eta_r)}\right)-\left(\frac{\omega_{ci}I_1e^{-bi}}{\omega-\omega_{ci}}\right)+\left(\frac{i\beta_r}{(\omega+i\eta_r)}\frac{n_{e0}}{n_{i0}}\right)-\left(\frac{\omega_{ci}I_1e^{-bi}}{\omega-\omega_{ci}}\right)\left(\frac{i\beta_r}{(\omega+i\eta_r)}\frac{n_{e0}}{n_{i0}}\right)-\frac{\omega_{pdr}^2}{S\omega^2}$$

$$=-\frac{1}{S}\left[\frac{\alpha_2}{A_1}+\frac{B_1}{C_1}\right]$$

$$1+\frac{T_i}{(1+\Delta_r)T_e}\left(\frac{i\beta_r}{(\omega+i\eta_r)}\right)-\left(\frac{1}{1+\Delta_r}\right)\left(\frac{\omega_{ci}I_1e^{-bi}}{\omega-\omega_{ci}}\right)$$

$$+\left(\frac{1}{1+\Delta_r}\right)\left(\frac{i\beta_r}{(\omega+i\eta_r)}\frac{n_{e0}}{n_{i0}}\right)-\left(\frac{1}{1+\Delta_r}\right)\left(\frac{\omega_{ci}I_1e^{-bi}}{\omega-\omega_{ci}}\right)\left(\frac{i\beta_r}{(\omega+i\eta_r)}\frac{n_{e0}}{n_{i0}}\right)-\left(\frac{1}{(1+\Delta_r)S}\right)\frac{\omega_{pdr}^2}{\omega^2}$$

$$=-\frac{1}{(1+\Delta_r)S}\left[\frac{\alpha_2}{A_1}+\frac{B_1}{C_1}\right]$$

Multiply by $\omega^2(\omega-\omega_{ci})(\omega+i\eta_r)$ on both sides, we get

$$\omega^2(\omega-\omega_{ci})(\omega+i\eta_r)+\omega^2(\omega-\omega_{ci})\left(\frac{T_i}{(1+\Delta_r)T_e}i\beta_r\right)$$

$$-\left(\frac{1}{1+\Delta_r}\right)\left(\omega^2(\omega+i\eta_r)\omega_{ci}I_1e^{-bi}\right)+\left(\frac{\omega^2(\omega-\omega_{ci})}{1+\Delta_r}\right)\left(i\beta_r\frac{n_{e0}}{n_{i0}}\right)$$

$$-\left(\frac{1}{1+\Delta_r}\right)\left(\omega^2\omega_{ci}I_1e^{-bi}\right)\left(i\beta_r\frac{n_{e0}}{n_{i0}}\right)-\left(\frac{(\omega-\omega_{ci})(\omega+i\eta_r)}{(1+\Delta_r)S}\right)\omega_{pdr}^2$$

$$=-\frac{\omega^2(\omega-\omega_{ci})(\omega+i\eta_r)}{(1+\Delta_r)S}\left[\frac{\alpha_2}{A_1}+\frac{B_1}{C_1}\right]$$

$$\left[\omega^2\left(\omega-\omega_{ci}\right)-\left(\frac{\omega^2\omega_{ci}I_1e^{-bi}}{1+\Delta_r}\right)-\left(\frac{\left(\omega-\omega_{ci}\right)}{\left(1+\Delta_r\right)S}\right)\omega_{pdr}^2\right]\left(\omega+i\eta_r\right)$$

$$+\omega^2\left(\omega-\omega_{ci}\right)\left(\frac{T_i}{\left(1+\Delta_r\right)T_e}i\beta_r\right)+\left(\frac{\omega^2\left(\omega-\omega_{ci}\right)}{1+\Delta_r}\right)\left(i\beta_r\frac{n_{e0}}{n_{i0}}\right)$$

$$-\left(\frac{1}{1+\Delta_r}\right)\left(\omega^2\omega_{ci}I_1e^{-bi}\right)\left(i\beta_r\frac{n_{e0}}{n_{i0}}\right)$$

$$=-\frac{\omega^2\left(\omega-\omega_{ci}\right)\left(\omega+i\eta_r\right)}{\left(1+\Delta_r\right)S}\left[\frac{\alpha_2}{A_1}+\frac{B_1}{C_1}\right]$$

Here we assume $\left(\omega-\omega_{ci}\right)=\omega_{ci}I_1e^{-bi}$, $\left(1+\Delta_r\right)\approx1$

$$\left(-\frac{\omega_{pdr}^2}{S}\right)\left(\omega+i\eta_r\right)+\left(\frac{\omega^2T_i}{T_e}i\beta_r\right)=-\frac{\omega^2\left(\omega+i\eta_r\right)}{S}\left[\frac{\alpha_2}{A_1}+\frac{B_1}{C_1}\right]$$

$$\left(-\frac{\omega_{pdr}^2}{S}\right)\left[\left(\omega+i\eta_r\right)-\left(\frac{S\omega^2T_i}{\omega_{pd}^2T_e}i\beta_r\right)\right]=-\frac{\omega^2\left(\omega+i\eta_r\right)}{S}\left[\frac{\alpha_2}{A_1}+\frac{B_1}{C_1}\right]$$

$$D=\left(\frac{T_i}{T_e}\beta_r\right)$$

$$\left[\left(\omega+i\eta_r\right)-\left(\frac{S\omega^2D}{\omega_{pdr}^2}i\right)\right]=\frac{\omega^2\left(\omega+i\eta_r\right)}{\omega_{pdr}^2}\left[\frac{\alpha_2}{A_1}+\frac{B_1}{C_1}\right]$$

$$\left[\omega+i\left(\eta_r-\frac{DS}{\omega_{pdr}^2}\omega^2\right)\right]=\frac{\omega^2\left(\omega+i\eta_r\right)}{\omega_{pdr}^2}\left[\frac{\alpha_2}{A_1}+\frac{B_1}{C_1}\right]$$

$$F=\left(\eta_r-\frac{DS}{\omega_{pdr}^2}\omega^2\right)$$

$$\left[\omega+iF\right]=\frac{\omega^2\left(\omega+i\eta_r\right)}{\omega_{pdr}^2}\left[\frac{\alpha_2}{A_1}+\frac{B_1}{C_1}\right]$$

$$\left[\omega+iF\right]\left[\omega-iF\right]=\left[\omega-iF\right]\frac{\omega^2\left(\omega+i\eta_r\right)}{\omega_{pdr}^2}\left[\frac{\alpha_2}{A_1}+\frac{B_1}{C_1}\right]$$

$$\omega^2+F^2=\left[\omega-iF\right]\frac{\omega^2\left(\omega+i\eta_r\right)}{\omega_{pdr}^2}\left[\frac{\alpha_2}{A_1}+\frac{B_1}{C_1}\right]$$

$$F^2=\eta_r^2+\left(\frac{DS}{\omega_{pdr}^2}\right)^2\omega^4-\left(2\eta_r\frac{DS}{\omega_{pdr}^2}\right)\omega^2$$

$$\omega^2+\eta_r^2+\left(\frac{DS}{\omega_{pdr}^2}\right)^2\omega^4-\left(2\eta_r\frac{DS}{\omega_{pdr}^2}\right)\omega^2=[\omega-iF]\frac{\omega^2\ (\omega+i\eta_r)}{\omega_{pdr}^2}\left[\frac{\alpha_2}{A_1}+\frac{B_1}{C_1}\right]$$

$$G=\left(\frac{DS}{\omega_{pdr}^2}\right)^2\ ,H=\left(2\eta_r\frac{DS}{\omega_{pdr}^2}\right)$$

$$\omega^2+\eta_r^2+G\omega^4-H\omega^2=[\omega-iF]\frac{\omega^2\ (\omega+i\eta_r)}{\omega_{pdr}^2}\left[\frac{\alpha_2}{A_1}+\frac{B_1}{C_1}\right]$$

$$\omega^4+\left(\frac{1-H}{G}\right)\omega^2+\frac{\eta_r^2}{G}=[\omega-iF]\frac{\omega^2\ (\omega+i\eta_r)}{G\omega_{pdr}^2}\left[\frac{\alpha_2}{A_1}+\frac{B_1}{C_1}\right]$$

$$\omega^4+I\omega^2+\frac{\eta_r^2}{G}=[\omega-iF]\frac{\omega^2\ (\omega+i\eta_r)}{G\omega_{pdr}^2}\left[\frac{\alpha_2}{A_1}+\frac{B_1}{C_1}\right]$$

$$\omega^4+I\omega^2+\frac{\eta_r^2}{G}=0$$

$$\omega^2=\frac{-I\pm\sqrt{I^2-4\frac{\eta_r^2}{G}}}{2}$$

$$\omega_{r1}^2=\frac{-I+\sqrt{I^2-4\frac{\eta_r^2}{G}}}{2}$$

$$\omega_{r2}^2=\frac{-I+\sqrt{I^2-4\frac{\eta_r^2}{G}}}{2}$$

$$\left(\omega^2-\omega_{r1}^2\right)\left(\omega^2-\omega_{r2}^2\right)=[\omega-iF]\frac{\omega^2\ (\omega+i\eta_r)}{G\omega_{pdr}^2}\left[\frac{\alpha_2}{A_1}+\frac{B_1}{C_1}\right]$$

$\omega=\omega_{r1}+\delta_1=\omega=k_zV_{0bz}+\omega_{cbr}+\delta_1$, where δ_1 is the small frequency mismatch.

When coupling coefficient is very large then

$$\omega_{r1}=\frac{\omega_0}{2}\left(\alpha_{3r}+\beta_{3r}\right)$$

$$\omega_{r2}=\frac{\omega_0}{2}\left(\alpha_{3r}-\beta_{3r}\right)$$

$$\left(\omega^2-\omega_{r1}^2\right)\left(\omega^2-\omega_{r2}^2\right)\left(\omega-k_zV_{0bz}-\omega_{cbr}\right)^2=[\omega-iF]\frac{\omega^2\ (\omega+i\eta_r)}{G\omega_{pdr}^2}[\alpha_2+B_1]$$

$$2\omega_{r1}\delta_1\left(\omega_{r1}^2-\omega_{r2}^2\right)\delta_1^2=[\omega_{r1}-iF]\frac{\omega_{r1}^2\ (\omega_{r1}+i\eta_r)}{G\omega_{pdr}^2}[\alpha_2+B_1]$$

$$\delta_1^3 = \frac{\left[\omega_{r1} - iF\right]}{2\omega_{r1}\left(\omega_{r1}^2 - \omega_{r2}^2\right)} \frac{\omega_{r1}^2\ \left(\omega_{r1} + i\eta_r\right)}{G\omega_{pdr}^2}\left[\alpha_2 + B_1\right]$$

$$\delta_1^3 = \frac{\left[\omega_{r1} - iF\right]}{2\left(\omega_{r1}^2 - \omega_{r2}^2\right)} \frac{\omega_{r1}\left(\omega_{r1} + i\eta_r\right)}{G\omega_{pdr}^2}\left[\alpha_2 + B_1\right]e^{i2\pi n}$$

$$\delta_1 = \left[\frac{\left[\omega_{r1} - iF\right]}{2\left(\omega_{r1}^2 - \omega_{r2}^2\right)} \frac{\omega_{r1}\ \left(\omega_{r1} + i\eta_r\right)}{G\omega_{pdr}^2}\left[\alpha_2 + B_1\right]\right]^{\frac{1}{3}} e^{\frac{i2\pi n}{3}}$$

$$P = \left[\frac{\left[\omega_{r1} - iF\right]}{2\left(\omega_{r1}^2 - \omega_{r2}^2\right)} \frac{\omega_{r1}\ \left(\omega_{r1} + i\eta_r\right)}{G\omega_{pdr}^2}\left[\alpha_2 + B_1\right]\right]$$

$$\delta_1 = \left[P\right]^{\frac{1}{3}}\left[-\frac{1}{2} + i\frac{\sqrt{3}}{2}\right]$$

$$\text{Growth rate}\left|\gamma\right| = \text{Img}\left[\delta_1\right] = \frac{\sqrt{3}}{2}\left[P\right]^{\frac{1}{3}}$$

$$\text{Growth rate}\left|\gamma\right| = \frac{\sqrt{3}}{2}\left[\frac{\left[\omega_{r1} - i\left(\eta_r - \frac{\beta_r \frac{T_i}{T_e}\left(\frac{2\omega_{pir}^2}{k^2 V_{thir}^2}\right)\omega_{r1}^2}{\omega_{pdr}^2}\right)\right]}{2\left(\omega_{r1}^2 - \omega_{r2}^2\right)\left(\beta_r \frac{T_i}{T_e}\right)^2\left(\frac{2\omega_{pir}^2}{k^2 V_{thir}^2}\right)^2}\omega_{r1}\omega_{pdr}^2\left(\omega_{r1} + i\eta_r\right)\left[\alpha_2 + \frac{\mu_r\omega_0^2\frac{\alpha_{3r}}{2}}{\left(1 + \frac{\omega_{pr}^2}{\omega_{cr}^2}\right)}\right]\right]^{\frac{1}{3}}$$

Chapter 6

RESULT AND DISCUSSION

I have done numerical calculations for the following dusty plasma parameter:

electron plasma density $n_{e0} = 10^9 cm^{-3}$,

ion plasma density $n_{i0} = 10^9 - 5\times10^5 cm^{-3} (\delta = 1-5)$,

dust grain density $n_{d0r} = 5\times10^5 cm^{-3}$,

electron temperature $T_e = 2eV$,

ion temperature $T_i = 1.5eV$,

dust grain size $a = 1-5\mu m$,

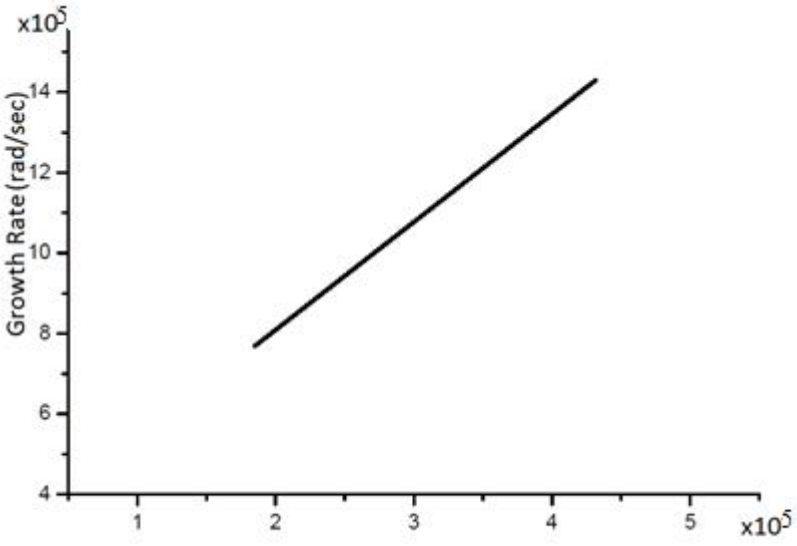

Grain Density n_{d0r}

Fig. 6.1 Growth rate (rad/sec) vs. Dust grain density n_{d0r}

From fig. 6.1, we can say that the growth rate γ (rad/sec) linearly increase with dust grain density n_{d0r}.

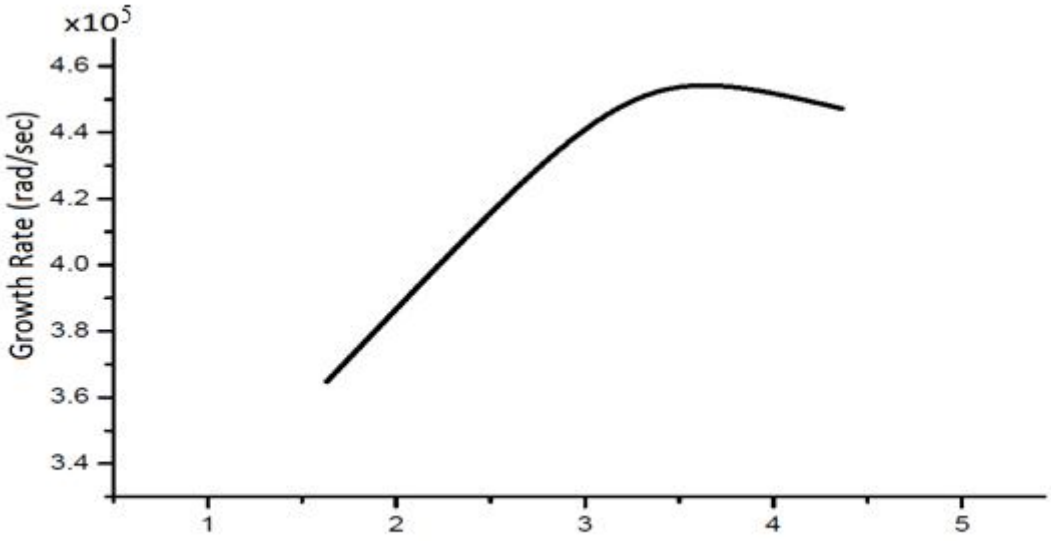

Fig. 6.2 Growth rate (rad/sec) vs. Relative density of dust grains δ

Relative density of dust grains $\delta\left(=\frac{n_{i0}}{n_{e0}}\right)$

From fig.6.2, it can be seen that the growth rate increases with the relative density of dust grains δ .

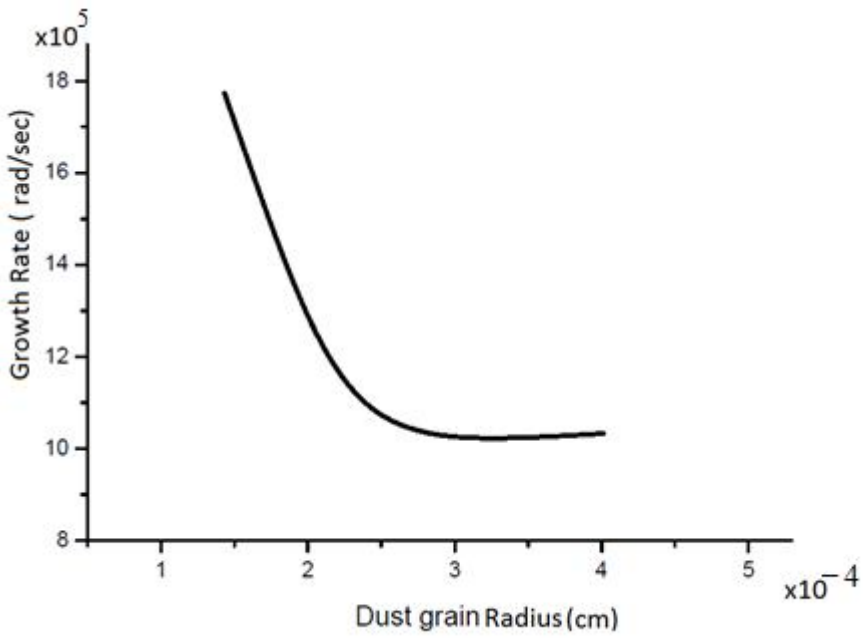

Fig. 6.3 Growth rate (rad/sec) vs. Dust grains size a (cm)

From fig.6.3, it can be seen that the growth rate increases with reducing the dust grain size.

REFERENCES

1. N. J. Fisch,Rev. Mod. Phys.59, 175, 1987.

2. V. Mukhovatov, M. Shimada, A. N.Chudnovskiyet al., Plasma Phys .Controlled Fusion45, A235, 2003.

3. ITER Physics Expert Group on Energetic Particles, Heating and Current Driveet al., Nucl. Fusion39, 2495, 1999.

4. M. Porkolab, J. J. Schuss, B. Lloydet al., Phys. Rev. Lett.53, 450, 1984.

5. Y. Ikeda, O. Naito, K. Ushigusa, M. Sato, T. Kondoh, S. Ide, M. Seki, K. Agashima, S. W. Wolfe, N. Asakura, M. Nemoto, and T. Imai,Nucl. Fusion34, 871, 1994.

6. F. X. Söldner, Proceedings of the 15th International Conference on Plasma Physics and Controlled Nuclear Fusion Research, Seville, 1994. IAEA, Vienna, 1995, Vol. 1, p. 423.

7. Y. Okumura, Y. Fujiwara, M. Kashiwagiet al., Rev. Sci. Instrum.71, 1219, 2000.

8. N. Umeda, L. R. Grisham, T. Yamamotoet al., Nucl. Fusion43, 522, 2003.

9. M. Kuriyama, N. Akino, N. Ebisawaet al., Fusion Sci. Technol. 42, 410, 2002.

10. T. Oikawa., 17th IAEA Conference on Fusion Energy IAEA, Yokohama, 1998, IAEA-F1-CN-69/CD/1.

11. H. W. Hendel, M. Yamada, S. W. Seiler, and H. Ikezi,Phys. Rev. Lett.36,319,1976.

12. G. A. Cottrell and R. O. Dendy,Phys. Rev. Lett.60,33,1988.

13. R. O. Dendy,Plasma Phys. Controlled Fusion36, B163, 1994.

14. R. O. Dendy, K. G. McClements, C. N. Lashmore-Davieset al., Phys. Plasmas1, 3407, 1994.

15. R. O. Dendy, K. G. McClements, C. N. Lashmore-Davieset al., Nucl.Fusion35, 1733, 1995.

16. K. G. McClements, C. Hunt, R. O. Dendy, and G.A.Cottrell,Phys.Rev.Lett.82,2099,1999.

17. H. Okuda, M. Ashour-Abdalla, and A. Miura,Geophys. Res. Lett.10,353, DOI: 10.1029/GL010i004p00353,1983.

18. N. S. Wolf, R. Majeski, H. Lashinsky, V. Tripathi, and C. S. Liu,Phys.Rev. Lett.45, 799, 1980.

19. G. S. Lakhina,Sol. Phys.57, 467,1978.

20. J. R. Myra and C. S. Liu,Phys. Rev. Lett.43, 861,1979.

21. C. S. Liu and V. K. Tripathi,Phys. Fluids23B, 345,1980.

22. C. S. Liu, V. K. Tripathi, V. S. Chan, and V. Stefan,Phys. Fluids27, 1709,1984.

23. V. N. Laxmi and V. K. Tripathi,Phys. Fluids30, 1485,1987.

24. G. Praburam, V. K. Tripathi, and V. K. Jain,Phys. Fluids31, 3145,1988.
25. R. Gore, J. Grun, and H. Lashinsky,Phys. Rev. Lett.40,1140, 1978.
26. G. Praburam, V. K. Tripathi, and G. Mishra,Phys. Rev. A43,968,1991.
27. K. G. McClements, R. O. Dendy, C. N. Lashmore-Davieset al., Phys. Plasmas3,543,1996.
28. A. G. Shalashov, E. V. Suvorov, and L. V. Lubyako,Plasma Phys. Controlled Fusion 45, 395 ,2003.
29. F. X. Soldner, V. Mertens, and R. Bartiromo,Plasma Phys. ControlledFusion33, 405, 1993.
30. C. S. Liu and V. K. Tripathi,Interaction of Electromagnetic Waves with Electron Beams and PlasmasWorld Scientific, Singapore, 1994,p115.
31. V. G. Panchenko, V. N. Pavlenko, E. Naslund, and L. Stenflo,Phys. Scr.31, 594,1985.
32. C. S. Liu and V. K. Tripathi,Phys. Rep.130, 143,1986.
33. Ashok Kumar and V. K. Tripathi, Physics of Plasmas 15, 062509 (2008).
34. M. R. Jana, A. Sen, and P. K. Kaw,Phys. Rev. E48, 3930,1993.
35. M. Mikikian and L. Boufendi,Phys. Plasmas11, 3733,2000.
36 .A. Bouchoule,Dusty Plasmas: Physics, Chemistry and Technological impacts in Plasma Processing!Wiley, New York, 1999.
37. K. Schonert, K. Eichas, and F. Niermoller,Powder Technol. 86, 41,1996.
38. A. P. Nefedov, G. E. Morfill, V. E. Fortov, H. M. Thomas, H. Rothermel,T. Hagl, A. V. Ivlev, M. Zuzic, B. A. Klumov, A. M. Lipaev, V. I. Molotkov, O. F. Petrov, Y. P. Gidzenko, S. K. Krikalev, W. Shepherd, A. I.Ivanov, M. Roth, H. Binnenbruck, J. A. Goree, and Y. P. Semenov,New J.Phys.5, 33,2003.
39. A. Bouchoule and L. Boufendi,Plasma Sources Sci. Technol. 2, 204,1993.
40. M. Cavarroc, M. C. Jouanny, K. Radouane, M. Mikikian, and L. Boufendi, J. Appl. Phys. 99, 064301, 2006.
41. M. Mikikian, L. Boufendi, A. Bouchoule, H. M. Thomas, G. E. Morfill, A.P. Nefedov, V. E. Fortov, and the PKE-Nefedov team,New J. Phys.5, 19,2003.
42. M. Mikikian and L. Boufendi,Phys. Plasmas11, 3733,2004.
43. S. Matsusaka, M. Oki, and H. Masuda, Powder Technol. 135–136, 150, 2003.
44. K. Schonert, K. Eichas, and F. Niermoller,Powder Technol. 86, 41,1996.
45. S. Anisimov, E. Mareev, N. Shikhova, A. Sorokin, and E. Dmitriev,Atmos. Res.76, 16 !2005".H. Kersten, H. Deutsch, and G. M. W. Kroesen, Int. J. Mass. Spectrom. 233, 51, 2004.
46. E. B. Tomme, D. A. Law, B. M. Annaratone, and J. E. Allen,Phys. Rev. Lett.85, 2518, 2000.

47. U. Konopka, F. Mokler, A. V. Ivlev,et al., 2005, “Charge-induced gelation of microparticles”,New J. Phys., vol. 7, p. 227.
48. P. K. Shukla and A. A. Mamun, 2002, Introduction to dusty plasma, IOP Publishing, Bristol.